AIAA 2004-2331, 2004

Fully Coupled Fluid-Structural Interactions Using an Efficient High Resolution Upwind Scheme

Xiangying Chen and Ge-Cheng Zha

Dept. of Mechanical and Aerospace Engineering
University of Miami
Coral Gables, Florida 33124

Background

• Fully coupled fluid-structure model is necessary to capture the nonlinear flow phenomena and structure coupling for turbomachinery flow induced vibration

• e.g.: Stall flutter have unsteady flow separation, shock motion, oscillating tip vortex, blade coupling in a bladed disk (IBR).

• Prescribed blade motion is difficult (inaccurate) if not impossible

Objective

• Achieve high CPU efficiency by using an efficient low diffusion E-CUSP scheme

Low Diffusion Upwind Schemes

• Roe's scheme, accurate, low diffusion, CPU intensive due to matrix operation.

• H-CUSP schemes, e.g. AUSM family schemes, efficient and accurate, pressure splitting is not fully consistent with characteristic direction.

• E-CUSP scheme, efficient and accurate, consistent with characteristic direction.

• The E-CUSP scheme recently suggested by Zha and Hu is employed.

CFD Aerodynamic Model

- Reynolds-Averaged Navier-Stokes equations(RANS)

$$\frac{\partial \mathbf{Q}'}{\partial \tau} + \frac{\partial \mathbf{Q}'}{\partial t} + \frac{\partial \mathbf{E}'}{\partial \xi} + \frac{\partial \mathbf{F}'}{\partial \eta} + \frac{\partial \mathbf{G}'}{\partial \zeta} = \frac{1}{Re}\left(\frac{\partial \mathbf{E}'_{\mathbf{v}}}{\partial \xi} + \frac{\partial \mathbf{F}'_{\mathbf{v}}}{\partial \eta} + \frac{\partial \mathbf{G}'_{\mathbf{v}}}{\partial \zeta}\right) \tag{1}$$

$$\mathbf{Q}' = \frac{\mathbf{Q}}{J} \tag{2}$$

$$\mathbf{E}' = \frac{1}{J}(\xi_t \mathbf{Q} + \xi_x \mathbf{E} + \xi_y \mathbf{F} + \xi_z \mathbf{G}) = \frac{1}{J}(\xi_t \mathbf{Q} + \mathbf{E}'') \tag{3}$$

$$\mathbf{F}' = \frac{1}{J}(\eta_t \mathbf{Q} + \eta_x \mathbf{E} + \eta_y \mathbf{F} + \eta_z \mathbf{G}) = \frac{1}{J}(\eta_t \mathbf{Q} + \mathbf{F}'') \tag{4}$$

$$\mathbf{G}' = \frac{1}{J}(\zeta_t \mathbf{Q} + \zeta_x \mathbf{E} + \zeta_y \mathbf{F} + \zeta_z \mathbf{G}) = \frac{1}{J}(\zeta_t \mathbf{Q} + \mathbf{G}'') \tag{5}$$

$$\mathbf{E}'_{\mathbf{v}} = \frac{1}{J}(\xi_x \mathbf{E}_{\mathbf{v}} + \xi_y \mathbf{F}_{\mathbf{v}} + \xi_z \mathbf{G}_{\mathbf{v}}) \tag{6}$$

$$\mathbf{F}'_{\mathbf{v}} = \frac{1}{J}(\eta_x \mathbf{E}_{\mathbf{v}} + \eta_y \mathbf{F}_{\mathbf{v}} + \eta_z \mathbf{G}_{\mathbf{v}}) \tag{7}$$

$$\mathbf{G}'_{\mathbf{v}} = \frac{1}{J}(\zeta_x \mathbf{E}_{\mathbf{v}} + \zeta_y \mathbf{F}_{\mathbf{v}} + \zeta_z \mathbf{G}_{\mathbf{v}}) \tag{8}$$

$$\mathbf{Q} = \begin{pmatrix} \bar{\rho} \\ \bar{\rho}\tilde{u} \\ \bar{\rho}\tilde{v} \\ \bar{\rho}\tilde{w} \\ \bar{\rho}\tilde{e} \end{pmatrix}, \mathbf{E} = \begin{pmatrix} \bar{\rho}\tilde{u} \\ \bar{\rho}\tilde{u}\tilde{u} + \tilde{p} \\ \bar{\rho}\tilde{u}\tilde{v} \\ \bar{\rho}\tilde{u}\tilde{w} \\ (\bar{\rho}\tilde{e} + \tilde{p})\tilde{u} \end{pmatrix},$$
$$\mathbf{F} = \begin{pmatrix} \bar{\rho}\tilde{v} \\ \bar{\rho}\tilde{u}\tilde{v} \\ \bar{\rho}\tilde{v}\tilde{v} + \tilde{p} \\ \bar{\rho}\tilde{w}\tilde{v} \\ (\bar{\rho}\tilde{e} + \tilde{p})\tilde{v} \end{pmatrix}, \mathbf{G} = \begin{pmatrix} \bar{\rho}w \\ \bar{\rho}\tilde{u}\tilde{w} \\ \bar{\rho}\tilde{v}\tilde{w} \\ \bar{\rho}\tilde{w}\tilde{w} + \tilde{p} \\ (\bar{\rho}\tilde{e} + \tilde{p})\tilde{w} \end{pmatrix},$$

$$\mathbf{E}'' = \xi_x \mathbf{E} + \xi_y \mathbf{F} + \xi_z \mathbf{G},$$

$$\mathbf{F}'' = \eta_x \mathbf{E} + \eta_y \mathbf{F} + \eta_z \mathbf{G},$$

$$\mathbf{G}'' = \zeta_x \mathbf{E} + \zeta_y \mathbf{F} + \zeta_z \mathbf{G},$$

$$\mathbf{E_v} = \begin{pmatrix} 0 \\ \bar{\tau}_{xx} - \overline{\rho u'' u''} \\ \bar{\tau}_{xy} - \overline{\rho u'' v''} \\ \bar{\tau}_{xz} - \overline{\rho u'' w''} \\ Q_x \end{pmatrix}, \; \mathbf{F_v} = \begin{pmatrix} 0 \\ \bar{\tau}_{yx} - \overline{\rho v'' u''} \\ \bar{\tau}_{yy} - \overline{\rho v'' v''} \\ \bar{\tau}_{yz} - \overline{\rho v'' w''} \\ Q_y \end{pmatrix},$$

$$\mathbf{G_v} = \begin{pmatrix} 0 \\ \bar{\tau}_{zx} - \overline{\rho w'' u''} \\ \bar{\tau}_{zy} - \overline{\rho w'' v''} \\ \bar{\tau}_{zz} - \overline{\rho w'' w''} \\ Q_z \end{pmatrix}$$

$$\bar{\tau}_{ij} = -\frac{2}{3}\tilde{\mu}\frac{\partial \tilde{u}_k}{\partial x_k}\delta_{ij} + \tilde{\mu}(\frac{\partial \tilde{u}_i}{\partial x_j} + \frac{\partial \tilde{u}_j}{\partial x_i}) \quad (9)$$

$$Q_i = \tilde{u}_j(\bar{\tau}_{ij} - \overline{\rho u'' u''}) - (\bar{q}_i + C_p \overline{\rho T'' u_i''}) \quad (10)$$

$$\bar{q}_i = -\frac{\tilde{\mu}}{(\gamma - 1)Pr}\frac{\partial a^2}{\partial x_i} \quad (11)$$

- Molecular viscosity $\tilde{\mu} = \tilde{\mu}(\tilde{T})$ is determined by Sutherland law

- Speed of sound $a = \sqrt{\gamma R T_\infty}$

- Total energy:

$$\bar{\rho}\tilde{e} = \frac{\tilde{p}}{(\gamma - 1)} + \frac{1}{2}\bar{\rho}(\tilde{u}^2 + \tilde{v}^2 + \tilde{w}^2) + k \quad (12)$$

- Turbulent shear stresses and heat flux are calculated
by Baldwin-Lomax model

Time Marching Scheme

Implicit unfactored line Gauss-Seidel iteration, dual time stepping

$$[(\frac{1}{\Delta\tau} + \frac{1.5}{\Delta t})I - (\frac{\partial R}{\partial Q})^{n+1,m}]\delta Q^{n+1,m+1} = R^{n+1,m} - \frac{3Q^{n+1,m} - 4Q^n + Q^{n-1}}{2\Delta t} \quad (13)$$

$$R = -\frac{1}{V}\int_s [(F - F_v)\mathbf{i} + (G - G_v)\mathbf{j} + (H - H_v)\mathbf{k}]\cdot d\mathbf{s} \quad (14)$$

The E-CUSP Scheme in Moving Mesh System

$$\mathbf{Q} = \begin{pmatrix} \bar\rho \\ \bar\rho\tilde u \\ \bar\rho\tilde v \\ \bar\rho\tilde w \\ \bar\rho\tilde e \end{pmatrix}, \quad \mathbf{E}' = \frac{1}{J}\hat{\mathbf{E}}, \quad \hat{\mathbf{E}} = \begin{pmatrix} \bar\rho\tilde U \\ \bar\rho\tilde u\tilde U + \xi_x\tilde p \\ \bar\rho\tilde v\tilde U + \xi_y\tilde p \\ \bar\rho\tilde w\tilde U + \xi_z\tilde p \\ \bar\rho\tilde e\tilde U + \tilde p\bar U \end{pmatrix} \tag{15}$$

contravariant velocity

$$\tilde U = \xi_t + \xi_x\tilde u + \xi_y\tilde v + \xi_z\tilde w \tag{16}$$

$\bar U$ defined as:

$$\bar U = \tilde U - \xi_t \tag{17}$$

$$\hat{\mathbf{E}} = \hat{\mathbf{A}}\mathbf{Q} = \hat{\mathbf{T}}\hat{\mathbf{\Lambda}}\hat{\mathbf{T}}^{-1}\mathbf{Q} \tag{18}$$

For E-CUSP scheme, the eigenvalue matrix is split as the following:

$$\hat{\mathbf{\Lambda}} = \begin{pmatrix} \tilde{U}-\tilde{C} & 0 & 0 & 0 & 0 \\ 0 & \tilde{U} & 0 & 0 & 0 \\ 0 & 0 & \tilde{U} & 0 & 0 \\ 0 & 0 & 0 & \tilde{U} & 0 \\ 0 & 0 & 0 & 0 & \tilde{U}+\tilde{C} \end{pmatrix} = \tilde{U}[\mathbf{I}] + \begin{pmatrix} -\tilde{C} & 0 & 0 & 0 & 0 \\ 0 & 0 & 0 & 0 & 0 \\ 0 & 0 & 0 & 0 & 0 \\ 0 & 0 & 0 & 0 & 0 \\ 0 & 0 & 0 & 0 & \tilde{C} \end{pmatrix} \tag{19}$$

$$\hat{\mathbf{E}} = \{\tilde{U}[\mathbf{I}\} + \begin{pmatrix} -\tilde{C} & 0 & 0 & 0 & 0 \\ 0 & 0 & 0 & 0 & 0 \\ 0 & 0 & 0 & 0 & 0 \\ 0 & 0 & 0 & 0 & 0 \\ 0 & 0 & 0 & 0 & \tilde{C} \end{pmatrix}]\mathbf{Q} = \hat{\mathbf{E}}^c + \hat{\mathbf{E}}^p = \begin{pmatrix} \bar{\rho}\tilde{U} \\ \bar{\rho}\tilde{u}\tilde{U} \\ \bar{\rho}\tilde{v}\tilde{U} \\ \bar{\rho}\tilde{w}\tilde{U} \\ \bar{\rho}\tilde{e}\tilde{U} \end{pmatrix} + \begin{pmatrix} 0 \\ \xi_x\tilde{p} \\ \xi_y\tilde{p} \\ \xi_z\tilde{p} \\ \tilde{p}\bar{U} \end{pmatrix} \tag{20}$$

Zha-Hu E-CUSP Scheme at Moving Grid

For subsonic flow, $M < 1$:

$$\hat{\mathbf{E}}_{\frac{1}{2}} = \frac{1}{2}[(\bar{\rho}\tilde{U})_{\frac{1}{2}}(\mathbf{q^c}_L + \mathbf{q^c}_R) - |\bar{\rho}\tilde{U}|_{\frac{1}{2}}(\mathbf{q^c}_R - \mathbf{q^c}_L)]$$
$$+ \begin{pmatrix} 0 \\ \mathcal{P}^+\tilde{p}\xi_x \\ \mathcal{P}^+\tilde{p}\xi_y \\ \mathcal{P}^+\tilde{p}\xi_z \\ \frac{1}{2}\tilde{p}(\bar{U} + \bar{C}_{\frac{1}{2}}) \end{pmatrix}_L + \begin{pmatrix} 0 \\ \mathcal{P}^-\tilde{p}\xi_x \\ \mathcal{P}^-\tilde{p}\xi_y \\ \mathcal{P}^-\tilde{p}\xi_z \\ \frac{1}{2}\tilde{p}(\bar{U} - \bar{C}_{\frac{1}{2}}) \end{pmatrix}_R \tag{21}$$

where

$$(\bar{\rho}\tilde{U})_{\frac{1}{2}} = (\bar{\rho}_L\tilde{U}_L^+ + \bar{\rho}_R\tilde{U}_R^-) \tag{22}$$

$$\mathbf{q^c} = \begin{pmatrix} 1 \\ \tilde{u} \\ \tilde{v} \\ \tilde{w} \\ \tilde{e} \end{pmatrix} \tag{23}$$

$$\tilde{C}_{\frac{1}{2}} = \frac{1}{2}(\tilde{C}_L + \tilde{C}_R) \tag{24}$$

$$\tilde{M}_L = \frac{\tilde{U}_L}{\tilde{C}_{\frac{1}{2}}}, \quad \tilde{M}_R = \frac{\tilde{U}_R}{\tilde{C}_{\frac{1}{2}}} \tag{25}$$

$$\tilde{U}_L^+ = \tilde{C}_{\frac{1}{2}}\{\frac{\tilde{M}_L + |\tilde{M}_L|}{2} + \alpha_L[\frac{1}{4}(\tilde{M}_L + 1)^2 - \frac{\tilde{M}_L + |\tilde{M}_L|}{2}]\} \tag{26}$$

$$\tilde{U}_R^- = \tilde{C}_{\frac{1}{2}}\{\frac{\tilde{M}_R - |\tilde{M}_R|}{2} + \alpha_R[-\frac{1}{4}(\tilde{M}_R - 1)^2 - \frac{\tilde{M}_R - |\tilde{M}_R|}{2}]\} \tag{27}$$

$$\alpha_L = \frac{2(\tilde{p}/\bar{\rho})_L}{(\tilde{p}/\bar{\rho})_L + (\tilde{p}/\bar{\rho})_R}, \quad \alpha_R = \frac{2(\tilde{p}/\bar{\rho})_R}{(\tilde{p}/\bar{\rho})_L + (\tilde{p}/\bar{\rho})_R} \tag{28}$$

$$\mathcal{P}^{\pm} = \frac{1}{4}(\tilde{M} \pm 1)^2(2 \mp \tilde{M}) \pm \alpha\tilde{M}(\tilde{M}^2 - 1)^2, \quad \alpha = \frac{3}{16} \tag{29}$$

$$\bar{C} = \tilde{C} - \xi_t \tag{30}$$

$$\bar{C}_{\frac{1}{2}} = \frac{1}{2}(\bar{C}_L + \bar{C}_R) \tag{31}$$

For supersonic flow,

when $\tilde{U}_L \geq \tilde{C}$, $\hat{\mathbf{E}}_{\frac{1}{2}} = \hat{\mathbf{E}}_L$

when $\tilde{U}_R \leq -\tilde{C}$, $\hat{\mathbf{E}}_{\frac{1}{2}} = \hat{\mathbf{E}}_R$

Boundary Conditions

• Upstream boundary conditions: All the variables are specified using freestream condition except the pressure is extrapolated from interior

• Downstream boundary conditions: All the variables are extrapolated from interior except the pressure is set to be its freestream value

• Solid wall boundary conditions: Non-slip condition

$$u_0 = 2\dot{x}_b - u_1, \qquad v_0 = 2\dot{y}_b - v_1 \tag{32}$$

and adiabatic and the inviscid normal momentum equation

$$\frac{\partial T}{\partial \eta} = 0, \quad \frac{\partial p}{\partial \eta} = -\left(\frac{\rho}{\eta_x^2 + \eta_y^2}\right)(\eta_x \ddot{x}_b + \eta_y \ddot{y}_b) \tag{33}$$

Geometric Conservation Law

$$\mathbf{S} = \mathbf{Q}\left[\frac{\partial J^{-1}}{\partial t} + \left(\frac{\xi_t}{J}\right)_\xi + \left(\frac{\eta_t}{J}\right)_\eta + \left(\frac{\zeta_t}{J}\right)_\zeta\right] \tag{34}$$

$$\mathbf{S}^{n+1} = \mathbf{S}^n + \frac{\partial \mathbf{S}}{\partial \mathbf{Q}}\Delta\mathbf{Q}^{n+1} \tag{35}$$

Structural model for elastic cylinder:

$$m\ddot{x} + C_x\dot{x} + K_x x = D \tag{36}$$

$$m\ddot{y} + C_y\dot{y} + K_y y = L \tag{37}$$

$C_x = C_y$ and $K_x = K_y$, After normalization:

$$\ddot{x} + 2\zeta\left(\frac{2}{\bar{u}}\right)\dot{x} + \left(\frac{2}{\bar{u}}\right)^2 x = \frac{2}{\mu_s\pi}C_d \tag{38}$$

$$\ddot{y} + 2\zeta\left(\frac{2}{\bar{u}}\right)\dot{y} + \left(\frac{2}{\bar{u}}\right)^2 y = \frac{2}{\mu_s\pi}C_l \tag{39}$$

$\zeta = \frac{C_{x,y}}{2\sqrt{mK_{x,y}}}$, $\bar{u} = \frac{U_\infty}{b\omega}$, $b = r$, $\omega = \sqrt{K_{x,y}/m}$, $\mu_s = \frac{m}{\pi\rho_\infty b^2}$,
C_d and C_l = Lift and drag coefficient

Matrix form:

$$[\mathbf{M}]\frac{\partial\{\mathbf{S}\}}{\partial t} + [\mathbf{K}]\{\mathbf{S}\} = \mathbf{q} \tag{40}$$

where

$$\mathbf{S} = \begin{pmatrix} x \\ \dot{x} \\ y \\ \dot{y} \end{pmatrix}, \mathbf{M} = [I],$$

$$\mathbf{K} = \begin{pmatrix} 0 & -1 & 0 & 0 \\ \left(\frac{2}{\bar{u}}\right)^2 & 2\zeta\left(\frac{2}{\bar{u}}\right) & 0 & 0 \\ 0 & 0 & 0 & -1 \\ 0 & 0 & \left(\frac{2}{\bar{u}}\right)^2 & 2\zeta\left(\frac{2}{\bar{u}}\right) \end{pmatrix}, \mathbf{q} = \begin{pmatrix} 0 \\ \frac{2}{\mu_s\pi}C_d \\ 0 \\ \frac{2}{\mu_s\pi}C_l \end{pmatrix}.$$

Time Marching:

$$\left(\frac{1}{\Delta\tau}\mathbf{I} + \frac{1.5}{\Delta t}\mathbf{M} + \mathbf{K}\right)\delta S^{n+1,m+1} = -\mathbf{M}\frac{3\mathbf{S}^{n+1,m} - 4\mathbf{S}^{n} + \mathbf{S}^{n-1}}{2\Delta t}$$
$$-\mathbf{K}\mathbf{S}^{n+1,m} + \mathbf{q}^{n+1,m+1} \tag{41}$$

Structural model for elastic airfoil:

$$m\ddot{h} + S_\alpha \ddot{\alpha} + K_h h = -L \tag{42}$$

$$S_\alpha \ddot{h} + I_\alpha \ddot{\alpha} + K_\alpha \alpha = M \tag{43}$$

Normalized:

$$\ddot{h} + x_\alpha \ddot{\alpha} + \left(\frac{\omega_h}{\omega_\alpha}\right)^2 h = -\frac{U^{*2}}{\mu\pi} C_l \tag{44}$$

$$x_\alpha \ddot{h} + r_\alpha^2 \ddot{\alpha} + r_\alpha^2 \alpha = \frac{U^{*2}}{\mu\pi} C_m \tag{45}$$

$U^* = \frac{U_\infty}{\omega_\alpha b}$,

Time scale: $t_s^* = \frac{\omega_\alpha L}{U_\infty} t_f^*$

Fully Coupled Fluid-Structural Interaction Procedure

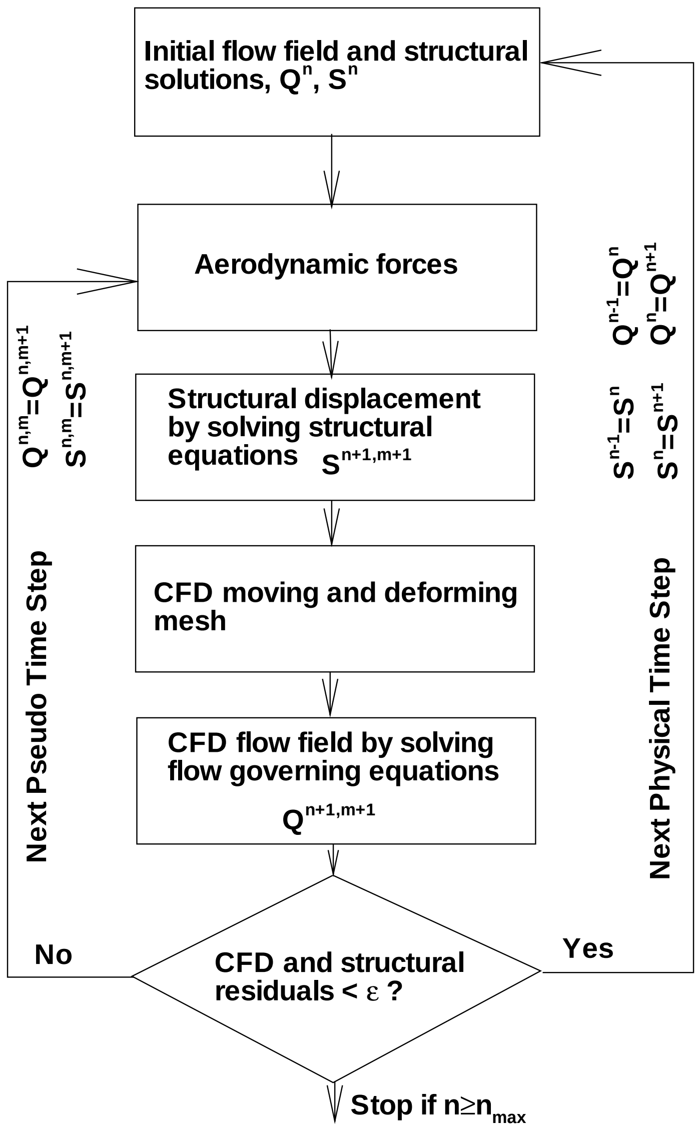

Figure 1: Flow-Structure Interaction Calculation Steps

- **Mesh Deformation Strategy**

1) inner zone: moving with the solid object, not deformed, keep the orthogonality and save CPU time

2) outer zone: moved with inner zone, deformed as a spring system, far field boundary stationary

Vortex-Induced Oscillating Cylinder

Re=500, M=0.2

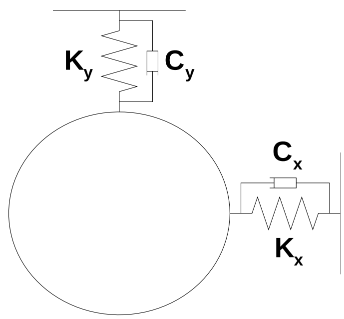

Figure 2: Sketch of the elastically mounted cylinder

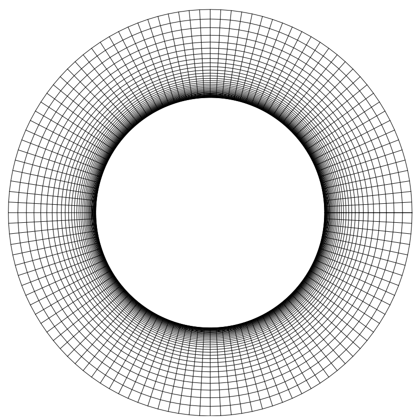

Figure 3: Mesh around the cylinder near the solid surface

Validation of Stationary cylinder vortex shedding

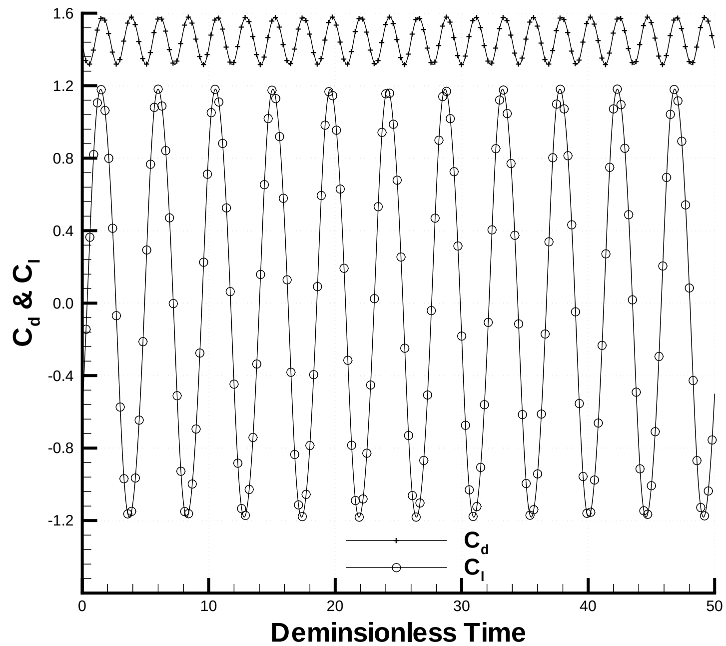

Figure 4: Time history of the lift and drag of the stationary cylinder due to vortex shedding

Table 1: Results of Mesh Refinement Study and comparison with the experiments

Mesh Dimension	St_{C_d}	St_{C_l}	St_{C_m}	C_l	C_d
120×80	0.4395	0.2197	0.2197	±1.1810	1.4529±0.1305
200×120	0.4516	0.2246	0.2246	±1.2267	1.4840±0.1450
(Roshko 1954)		0.2075			
(Goldstein 1938)		0.2066			
384×96 (Alonso 1995)	0.46735	0.23313		1.14946(C_{lmax})	1.31523(C_{davg})

Flow induced vibration

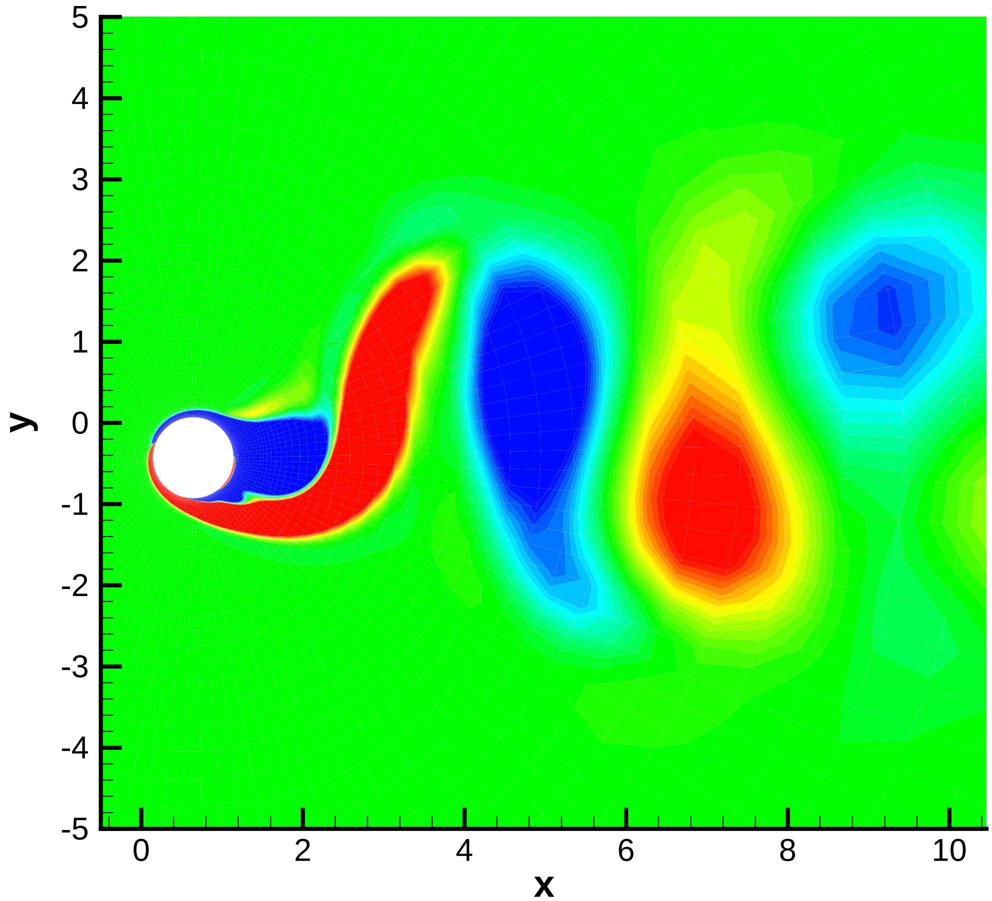

Figure 5: Vorticity contours with small cylinder structural oscillation amplitude, $\mu_s = 12.7322$, $\zeta = 0.03166$,

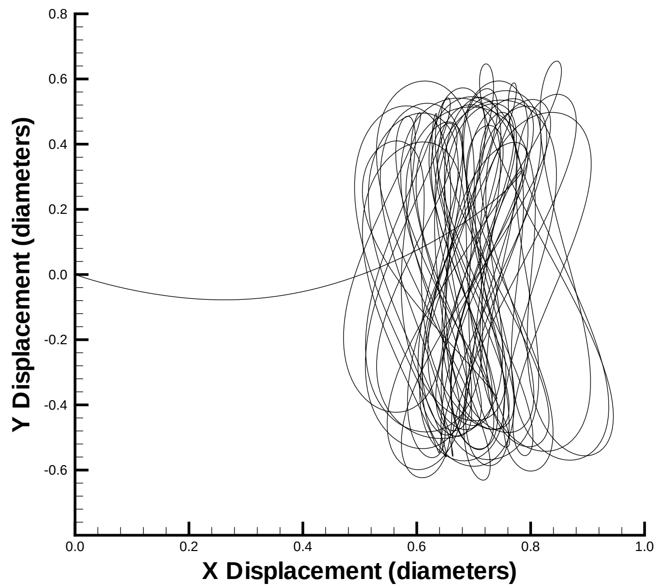

Figure 6: The trajectory of the Time histories of the lift and drag coefficients of the oscillating cylinder, $\mu_s = 1.2732$, $\zeta = 0.03166$

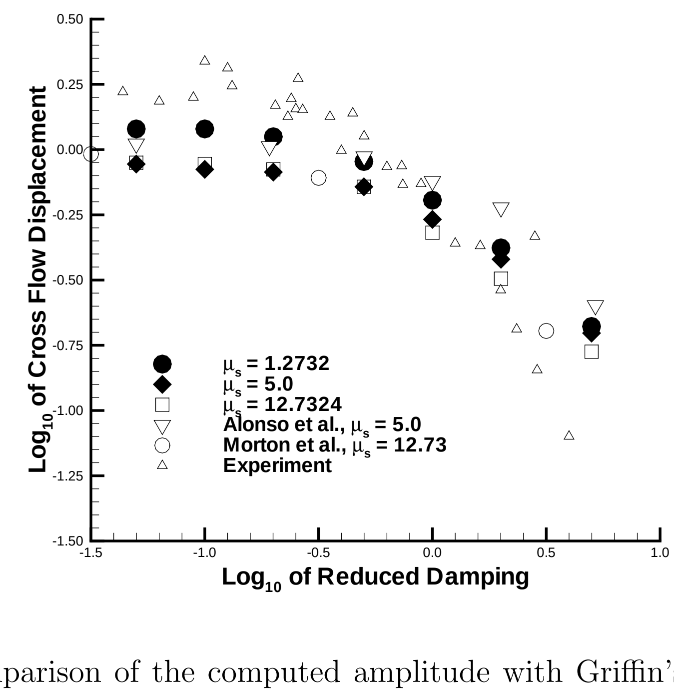

Figure 7: Comparison of the computed amplitude with Griffin's experimental data for the elastically mounted cylinder.

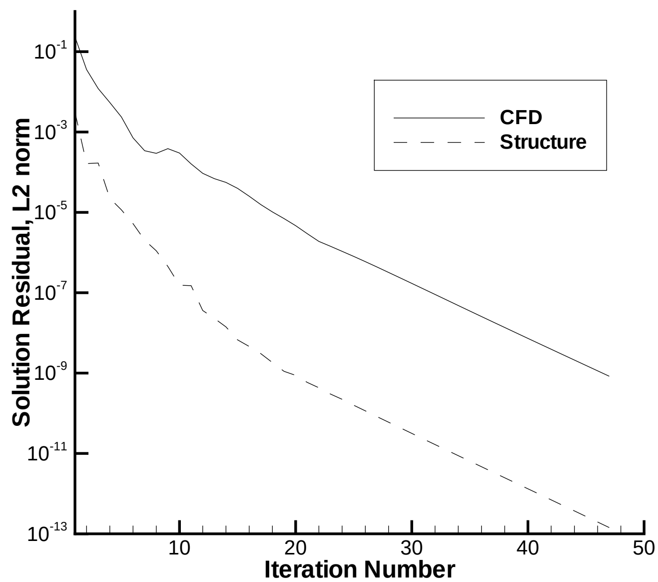

Figure 8: Convergence histories for both CFD and structural solvers within one physical time step

Steady State Flow of Transonic RAE 2822 Airfoil

Re=6.5×10^6, M_∞=0.729, AoA=2.31°.

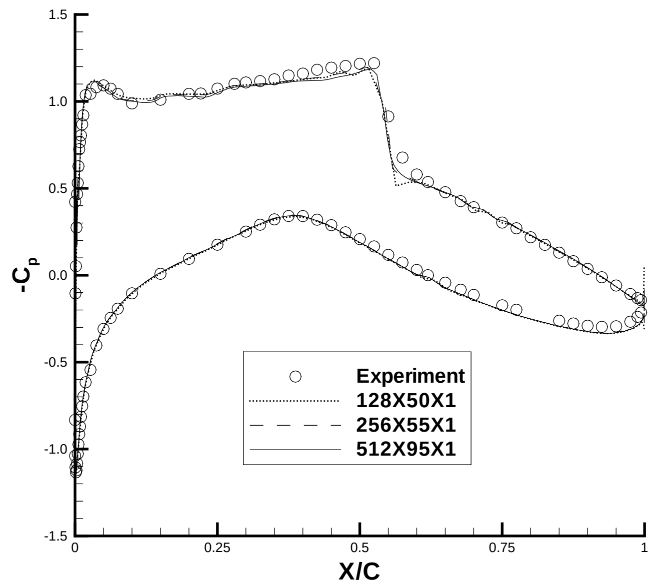

Figure 9: Pressure coefficient comparison

Table 2: Aerodynamic coefficients and $y+$ for RAE 2822 Airfoil

Mesh Dimension	C_d	C_l	C_m	$y+$
128×50	0.01482	0.73991	0.09914	0.0833 - 2.3864
256×55	0.01455	0.73729	0.09840	0.1318 - 2.4016
512×95	0.01426	0.74791	0.09994	0.2309 - 2.0228
Prananta et al.	0.01500	0.74800	0.09800	
Experiment	0.01270	0.74300	0.09500	

Forced Pitching NACA 64A010 Airfoil

Re=1.256×10^7, M_∞=0.8

$$\alpha(t) = \alpha_m + \alpha_o sin(\omega t) \tag{46}$$

$\alpha_m = 0$, $\alpha_o = 1.01°$

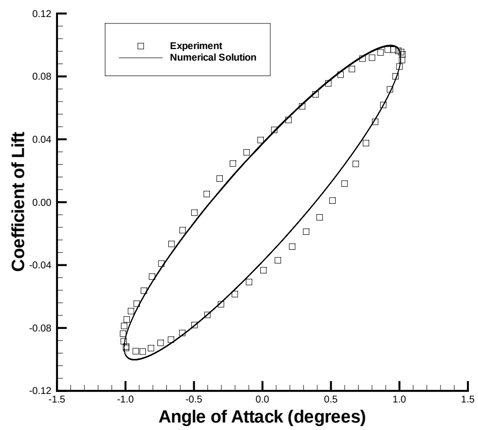

Figure 10: Comparison of computed lift coefficient with Davis' experimental data for the forced pitching airfoil.

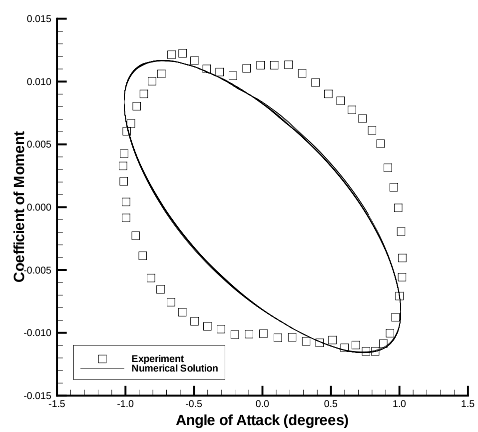

Figure 11: Comparison of computed moment coefficient with Davis' experimental data for the forced pitching airfoil.

Flutter Prediction for NACA 64A010 Airfoil

$Re = 1.256 \times 10^7$, $M_\infty = 0.75 - 0.95$, $a = -2.0$, $x_\alpha = 1.8$, $\frac{\omega_\alpha}{\omega_h} = 1$, $r_\alpha^2 = 3.48$, $\mu = 60$.

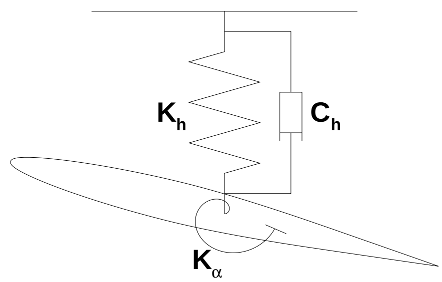

Figure 12: Sketch of the elastically mounted airfoil

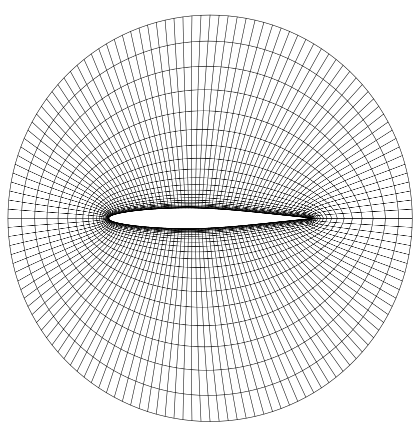

Figure 13: O-type mesh around the NACA 64A010 airfoil

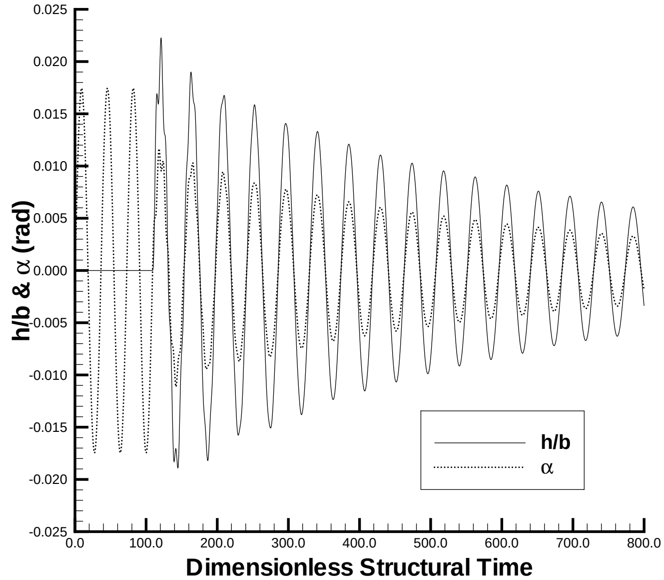

Figure 14: Time histories of plunging and pitching displacements for $M_\infty = 0.825$ and $V^* = 0.55$ - Damped response.

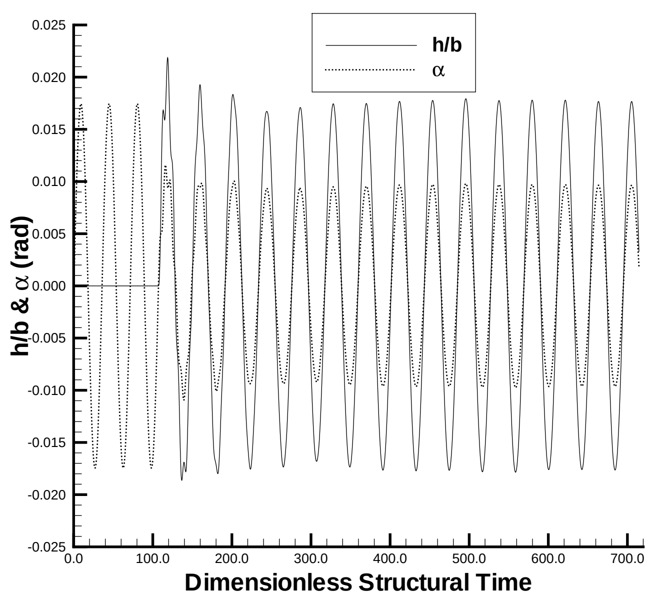

Figure 15: Time histories of plunging and pitching displacements for $M_\infty = 0.825$ and $V^* = 0.615$ - Neutrally stable response.

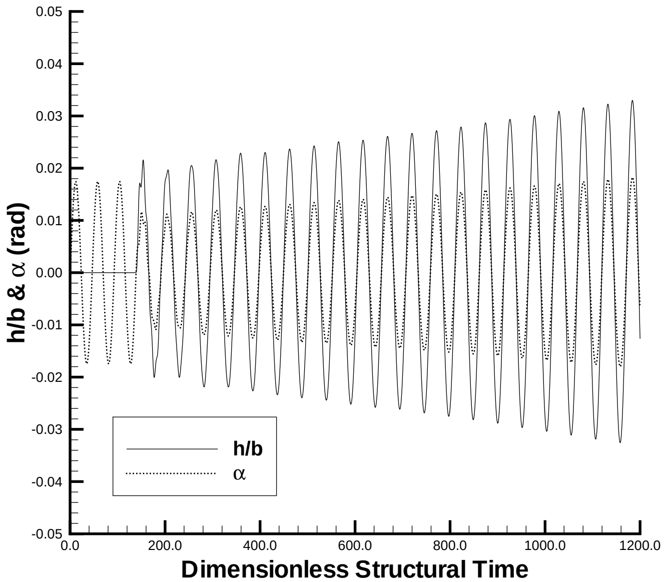

Figure 16: Time histories of plunging and pitching displacements for $M_\infty = 0.825$ and $V^* = 0.70$ - Diverging response.

Conclusion

• The efficient high resolution E-CUSP upwind scheme of Zha and Hu is extended to moving grid with fully coupled fluid-structural interaction.

• For an elastically mounted cylinder, computed cross-flow displacement of the cylinder agree well with experiment

• For the forced pitching NACA 64A010 airfoil, the computed lift oscillation agrees very well with the experiment The computed moment oscillation has large deviation from the experiment

• For the elastically mounted airfoil, the predicted flutter boundary agree well with the results of other researchers